International Journal of Immunopathology & Pharmacology

Original Research Article

Dissociation between the expression of cGAS/STING and a senescence-associated signature in colon cancer

International Journal of Immunopathology and Pharmacology
Volume 39: 1–14

DOI: 10.1177/03946320251324821
journals.sagepub.com/home/iji
Sage

Sofian Al Shboul[1], Ola Abu Al Karsaneh[2*], Moath Alrjoub[3*], Mohammad Al-Qudah[2,3], Mohammed El-Sadoni[4*], Ahmad Alhesa[4*], Mohannad Ramadan[1,5], Marwa Barukba[3*], Esraa Fares Al-Quran[3*], Amr Masaadeh[3,6*], Farah N Almasri[3], Uruk Shahin[1], Moureq R. Alotaibi[7], Mohammad Al-Azab[2], Ashraf I. Khasawneh[2,8] and Tareq Saleh[1,9]

Abstract

Objective: The effect of the cGAS/STING pathway on antitumor immunity and its connection to senescence in vivo necessitates further investigation.

Introduction: Cellular senescence and its secretory phenotype (the SASP) are implicated in modulating the immune microenvironment of cancer possibly through the cGAS/STING pathway.

Methods: Gene expression data from paired colon cancer and adjacent non-malignant mucosa (98 patients, $n = 196$ samples; 65 patients, $n = 130$ samples) were analyzed for cGAS/STING and a senescence signature. Immunohistochemistry assessed cGAS/STING protein expression in 124 colorectal samples.

Results: Approximately one-quarter of patients displayed senescence profiles in both gene sets, yet without significantly correlating with cGAS/STING expression. Notably, cGAS expression was higher than STING in tumor tissue compared to non-malignant colonic mucosa. Protein analysis showed 83% positive cGAS expression and 39% positive STING expression, with discrepancies in expression patterns. Additionally, 15% of samples lacked both markers, while 35% exhibited positive staining for both. No significant correlations were found between cGAS/STING status and tumor stage, patient age, lymphovascular invasion, or lymph node involvement.

[1]Department of Pharmacology and Public Health, Faculty of Medicine, The Hashemite University, Zarqa, Jordan
[2]Department of Microbiology, Pathology and Forensic Medicine, Faculty of Medicine, The Hashemite University, Zarqa, Jordan
[3]Department of Pathology and Microbiology, Faculty of Medicine, Jordan University of Science and Technology, Irbid, Jordan
[4]Department of Pathology, Microbiology and Forensic Medicine, School of Medicine, The University of Jordan, Amman, Jordan
[5]Trinity Centre for Global Health, Trinity College Dublin, Dublin, Ireland
[6]Department of Pathology, University of Iowa Hospitals & Clinics, Iowa City, IA, USA
[7]Department of Pharmacology and Toxicology, College of Pharmacy, King Saud University, Riyadh, Saudi Arabia
[8]Department of Laboratory Medicine, National Institutes of Health Clinical Center, Bethesda, MD, USA
[9]Department of Pharmacology & Therapeutics, College of Medicine & Health Sciences, Arabian Gulf University, Manama, Bahrain

*These authors contributed equally to this work.

Corresponding authors:
Sofian Al Shboul, Department of Pharmacology and Public Health, Faculty of Medicine, The Hashemite University, Zarqa 13133, Jordan.
Email: sofian@hu.edu.jo

Tareq Saleh, Department of Pharmacology and Public Health, Faculty of Medicine, The Hashemite University, Damascus Highway, Zarqa 13133, Jordan; Department of Pharmacology & Therapeutics, College of Medicine & Health Sciences, Arabian Gulf Uni-versity, Manama, Bahrain.
Emails: tareq@hu.edu.jo; tareqnrs@agu.edu.bh

Conclusions: Our findings demonstrate significant senescence marker expression in colorectal cancer samples but with no correlation with cGAS/STING.

Keywords
colon cancer, cGAS, STING, SASP, senescence

Date received: 23 August 2024; accepted: 13 February 2025

Introduction

Cellular senescence is a unique cell fate characterized by a stable growth arrest.[1,2] Senescent cells exhibit distinctive phenotypes including cellular hypertrophy, reduced nucleocytoplasmic ratio,[3,4] mitochondrial dysfunction,[5] increased oxidative burden,[6] and macromolecular damage.[7,8] Senescent cells release a spectrum of factors into the microenvironment as a result of widespread gene expression changes in interferon-related, insulin growth factor-related, MAP kinase-related, and oxidative stress pathways.[9–11] Senescence represents a cardinal hallmark of cancer through its two arms: Oncogene-Induced Senescence (OIS) triggered in response to aberrant oncogenic signals,[12] and Therapy Induced Senescence (TIS) elicited in response to cancer treatments.[13] Senescence is initially tumor suppressive,[14] however, it can later contribute to proliferative recovery, stemness, and aggressive tumor cell behavior.[13,15] Senescent cells can also promote a pro-tumorigenic microenvironment through the secretion of certain members of the Senescence-Associated Secretory Phenotype (SASP) fostering chronic inflammation, remodeling of the extracellular matrix, and immunoevasion.[16]

The SASP contains various immunoactive molecules that can influence tumor-infiltrating immune cells. For example, senescent liver stellate cells are able to shift macrophage polarization towards antitumor M1 state,[17] while senescent thyrocytes trigger immunosuppressive M2 macrophage polarization.[18] Furthermore, single-cell transcriptomic analysis revealed that complement released from non-senescent tumor cells stimulates M1 differentiation and antigen presentation,[19] while senescent tumor cells secrete CCL20 to favor immunosuppressive M2 polarization in pancreatic cancer.[20] Furthermore, CCL2, a frequent SASP component, can trigger infiltration of natural killer (NK) cells into the tumor mass resulting in enhanced tumor cell elimination and, interestingly, elimination of senescent cells.[21,22] While some SASP components like IL-6 and IL-8 have been implicated in creating immunogenic milieu,[23] chronic inflammation driven by the SASP may foster tumor growth and metastasis by promoting angiogenesis and tissue remodeling.[11] Additionally, certain SASP factors can induce the expression of immune checkpoint molecules such as PD-L1 on tumor cells,[24] thereby enabling them to evade T-cell-mediated killing.[25] Further complexity of SASP's role in driving antitumor immunity is underscored by its ability to modulate the activity of regulatory T cells (Tregs) which can suppress effective antitumor responses.[26,27] Moreover, it was shown that senescent cells can utilize the HLA-E, a non-classical MHC molecule, to inhibit immune responses from NK and CD8+ T cells, thereby evading immunosurveillance.[28] Collectively, senescence seems to contribute unfavorably to tumor immunosurveillance, but this role requires further exploration.

The cyclic GMP-AMP synthase (cGAS) and Stimulator of Interferon Genes (STING) pathway is a crucial regulator of innate immune responses and plays a critical role in detecting cytoplasmic DNA (particularly from pathogens and damaged or stressed cells).[29] Activation of cGAS/STING leads to the production of type I interferons (IFNs) and other proinflammatory cytokines that orchestrate innate and adaptive immune responses.[30] The cGAS/STING pathway is activated in senescent cells and contributes to the establishment of the SASP.[31–33] Deletion of cGAS can significantly abrogate the SASP and facilitate escape from senescence.[31,34] Subsequently, cGAS/STING pathway contributes to the SASP-mediated immunomodulation of the tumor microenvironment,[35] and thus might facilitate the ability of senescent tumor cells to evade immunosurveillance.[36] However, the connection between the cGAS/STING pathway and development of senescence in vivo remains an unexplored area, especially that senescence is a major component of tumor biology in cancer patients.[37]

We utilized colon cancer as a model to examine the expression of cGAS/STING relative to senescence gene signatures. cGAS, but not STING, gene expression is increased in colon cancer tissue relative to its paired non-malignant mucosa with no correlation with senescence and is widely expressed at the protein level compared to STING. This work invites a more rigorous examination of the role that cGAS/STING plays in regulating senescence.

Materials and methods

Tissue samples

Formalin-fixed, paraffin-embedded (FFPE) tissue blocks of colon cancer were used to construct nine tissue microarray (TMA) slides each supposed to consist of 25 samples at the pathology department at King Abdullah University Hospital (KAUH) as previously described.[38,39] This study represents a retrospective analysis that included an independent, original sample of colon cancer patients diagnosed between the period 2004–2018 at KAUH. Three co-authors (M.B, E.F.A, A.M) confirmed the diagnosis and marked the slides for TMA construction. The staining of cGAS and STING was performed on nine TMA slides of colon cancer, each slide contained 25 cores, however, the final included data for analysis was 135 samples for cGAS and 133 cores for STING, the remaining cores were either missing, folded or did not show tumor regions.

Immunohistochemistry (IHC)

IHC was conducted based on established protocols with modifications tailored to this study.[40,41] Multiple 4-µm-thick sections were prepared from the TMA colon cancer blocks using a microtome (RM2235 rotary microtome, Leica Biosystems, Wetzlar, Germany). Sections were floated in a water bath at approximately 45°C and subsequently mounted on clean positively charged glass slides (Xtra Clipped Corner Slides, Leica Biosystems, Wetzlar, Germany). Slides were dried at 65°C for 30 min, then immersed in fresh xylene twice for 5 min each followed by graded ethanol rehydration series (100%, 95%, and 70% ethanol; 3 min each) and a brief rinse in deionized water. For antigen retrieval, slides were placed in jars containing sodium citrate buffer (pH 6.0) for cGAS or Tris–EDTA buffer (pH 9.0) for STING and heated in a water bath at 95°C for 20 min. After cooling at room temperature for 20 min, slides were rinsed twice with phosphate-buffered saline (PBS) containing 0.2% Tween 20 (CAS 9005-64-5, Sigma Al-drich, St. Louis, USA). Endogenous peroxidase activity was suppressed by treating slides with 3% hydrogen peroxide in PBS. After additional PBS rinse, sections were incubated with 5% bovine serum albumin (BSA) (Atlas Medical, Germany) for 1 h at room temperature to block non-specific binding.

The primary antibodies, anti-cGAS antibody (1:400, Cat. No. NBP1-86761, Novus biologicals, USA) and anti-STING antibody (1:400, ab227705, Abcam, Cambridge, United Kingdom) were applied to the slides and incubated for 2 h at room temperature. Following incubation, sections were rinsed in PBS and treated with a super enhancer reagent (Super Sensitive™ Polymer-HRP IHC Detection, QD440-XAKE, BioGenex, USA) for 25 min at room temperature for Poly-HRP signal. After another PBS wash, slides were further incubated with HRP-Polymer anti-Mouse/Rabbit reagent (Super Sensitive™ Polymer-HRP IHC Detection, QD440-XAKE, BioGenex, USA) for 30 min at room temperature. Immunostaining was visualized using 3, 3′-diaminobenzidine tetrahydrochloride (DAB) for 8 min. Counterstaining was performed using Mayer's hematoxylin solution, followed by 30 sec treatment with lithium carbonate solution. The slides were then dehydrated through a graded ethanol series (70%, 95%, and 100% ethanol; 3 min each), cleared in fresh xylene, and mounted with dibutyl phthalate in xylene (DPX) mounting media (#BCBX0183, Sigma, Germany).

cGAS and STING protein expression scoring

The diagnosis of colorectal adenocarcinoma was established at The Pathology Department at KAUH. Two independent pathologists (co-authors: MA and OAAK) conducted the pathological evaluation of the colon cancer samples and the immunohistochemical scoring of cGAS and STING protein expressions using a light microscope (Labo America, USA). In some cases, the tissue core did not show tumor regions, these cases were either excluded from the scores or were counted as normal if the tissue was agreed upon that represents normal mucosa. The IHC score for cGAS, and

STING were performed as previously described in the literature.[42,43] For both markers, immunostaining was assessed for cytoplasmic staining. First, the intensity of the cytoplasmic staining was scaled as follows: 0 (none), 1+ (weak), 2+ (moderate), or 3+ (strong) staining. Then, the extent of tumor cells showing cytoplasmic staining was given the following score (0: lack of staining, 1: <10%, 2: 10%–50%, and 3: >50% of tumor cells stained). The final score was calculated by multiplying the intensity score and the extent score, yielding a total score between 0 and 9. A final score of 3 or more was considered a positive expression.

Gene expression analysis

Two datasets of gene expression were obtained as normalized and processed RNA-seq data from the GEO database.[44] The first dataset (GSE44076: https://www.ncbi.nlm.nih.gov/geo/query/acc.cgi?acc=GSE44076) includes gene expression profiles from 98 patients newly diagnosed with microsatellite stable colorectal adenocarcinoma who had not undergone neoadjuvant chemotherapy, with both tumor and adjacent normal mucosa samples available.[45] The second dataset (GSE20842: https://www.ncbi.nlm.nih.gov/geo/query/acc.cgi?acc=GSE20842) comprises pretreatment biopsy from 65 patients with locally advanced rectal cancer[46]

Gene set enrichment analysis (GSEA)

Raw gene expression data were processed by mapping the probe IDs to gene symbols using the platform annotation file associated with the microarray data (GPL13667 for GSE44076 and GPL4133 for GSE20842). Mappings were verified and missing gene symbols were excluded. Data processing and mapping were performed using Python (pandas library).[47,48] Next, the phenotype file *(.cls)* was generated to specify the sample classifications (e.g. High vs Low senescence groups).[49] GSEA was conducted using the "gseapy" Python package.[50] Firstly, processed gene expression data and the (*.cls*) phenotype file were used as inputs. Several gene set collections obtained from the Molecular Signatures Database (MSigDB) were used to cover general pathways and interferon related-genes.[47,51] The sets used were: (1) "c2.all.v2024.1.Hs.symbols" which contains 5,504 genes; (2) "HALLMARK_INTERFERON_ALPHA_RESPONSE.v2024.1.Hs" that contain 97 genes associated with interferon-alpha signaling and its downstream effects in human; (3) "HALLMARK_INTERFERON_GAMMA_RESPONSE.v2024.1.Hs" which has 200 genes that represent the key pathways and processes activated by interferon-gamma signaling, including antigen processing and presentation, antiviral responses, and modulation of immune cell activity. GSEA was run using the signal-to-noise ratio as the ranking metric, with 1000 permutations of the phenotype labels. False Discovery Rate (FDR) was used to correct for multiple comparisons, and pathways with FDR *q*-values below 0.25 were considered significant.[47,52]

Statistical analysis

Gene expression and IHC analyses were conducted using SPSS version 25 and R studio. Differences between tumor and matched normal samples in each dataset were calculated to determine relative gene expression increases or decreases. Pearson chi-square (χ^2) or Fisher's exact (non-parametric test) was used to examine associations between cGAS and/or STING protein expression and clinicopathologic variables. We conducted the Shapiro-Wilk test to examine the normality of the gene expression datasets and found that they were normally distributed so performed Pearson Correlation Coefficient. All p values reported are two-tailed, statistical significance set at $p \leqslant 0.05$.

Results

cGAS, but not STING, is highly expressed in colon cancer tissue relative to matched normal mucosa

First, we sought to examine cGAS and STING gene expression levels using two publicly available gene expression datasets of colon cancer and its corresponding adjacent non-malignant mucosa obtained from the same patient (paired samples). The first set consisted of samples from 98 patients ($n=196$; GSE44076) and the other had 65 patients ($n=130$; GSE20842).[45,46] Less than half of the paired samples (45%, $n=44/98$) within the first set (GSE4-4076) exhibited increased levels of cGAS/STING

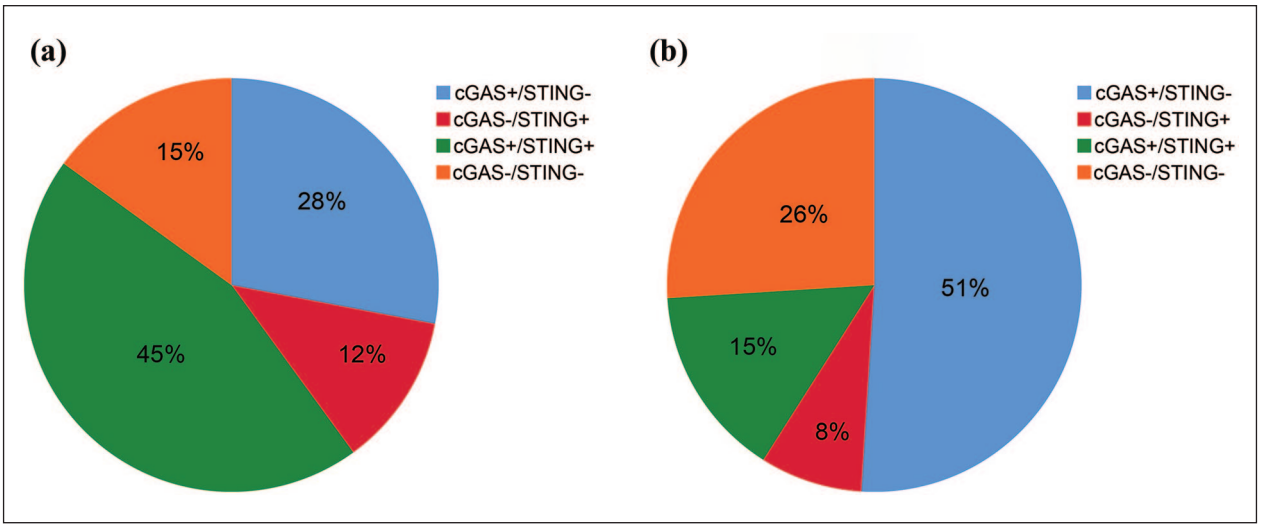

Figure 1. Pie chart graph showing the status of cGAS/STING as defined by the delta between colon tumor tissue and its paired normal mucosa in two gene expression datasets. (a) One had 98 patients (196 samples; GSE44076)[45] and the other (b) had 65 patients (130 sample; GSE20842).[46]
Positive change indicates expression was higher in tumor relative to normal and negative change is vice versa.

(↑cGAS/↑STING) gene expression in tumor tissue compared to its paired non-malignant mucosa (Figure 1(a)). However, this percentage was lower within the second set (GSE20842), whereas only 15% (n=10/65) exhibited a similar expression profile (Figure 1(b)). On the other hand, 15% (n=15/98) of the samples of the GSE44076 set showed reduced expression of both cGAS/STING (↓cGAS/↓STING), whilst 26% (n=17/65) of GSE20842 paired samples exhibited ↓cGAS/↓STING in tumor tissue relative to its matched non-malignant mucosa. Interestingly, the percentage of increased cGAS expression accompanied by decreased STING gene expression (↑cGAS/↓STING) was found in 28% (n=27/98) of GSE44076 samples (Figure 1(a)), and more than half of GSE20842 samples 51% (33/65) had a similar profile among the GSE20842 set (Figure 1(b)). The opposite profile of ↓cGAS/↑STING was found in just 12% (12/98) and 8% (5/65) of the samples within GSE44076 and GSE20842, respectively.

cGAS/STING gene expression is not connected to a senescence gene expression signature in colon cancer tissue samples

In order to investigate the association between of cGAS/STING gene expression change between tumor and matched non-malignant mucosa and senescence, we utilized a recently published senescence gene expression signature that relied on a set of seven genes (*IGFBP3*, *IGFBP7*, *BHLHE40*, *TTYH3*, *TIMP1*, *TAGLN*, and *PLOD3*).[49] IGFBP3 and IGFBP7 are both part of the insulin-like growth factor binding protein family and are typically involved in binding insulin-like growth factors in plasma, extending their half-lives and modulating their interaction with target cell surface receptors. Both proteins have been strongly identified as markers of senescence and aging (and are components of the SASP).[53–55] BHLHE40 (also known as differentiated embryo chondrocyte 1, DEC1) is a transcription factor belonging to the basic helix-loop-helix family that plays a role in regulating circadian rhythm, immune function, and cellular differentiation and has also been strongly associated with senescence.[56] TIMP1, an inhibitor of matrix metalloproteinases (MMPs), and TAGLN, an actin-binding protein primarily involved in the regulation of the cytoskeleton and smooth muscle cell differentiation, both have been linked to senescence.[57,58] Both TTYH3 and PLOD3 have been identified by Lv et al. as senescence markers.[49]

In our analysis, for a sample to be considered as possessing "high" senescence gene expression profile, all the seven genes should exhibit an increase in their gene expression level in tumor tissue compared to its matched adjacent non-malignant mucosa. Alternatively, any decrease in any of the seven genes was considered a breach of the signature and the sample was identified to have "low" senescence gene expression profile.[49] It is noteworthy that this

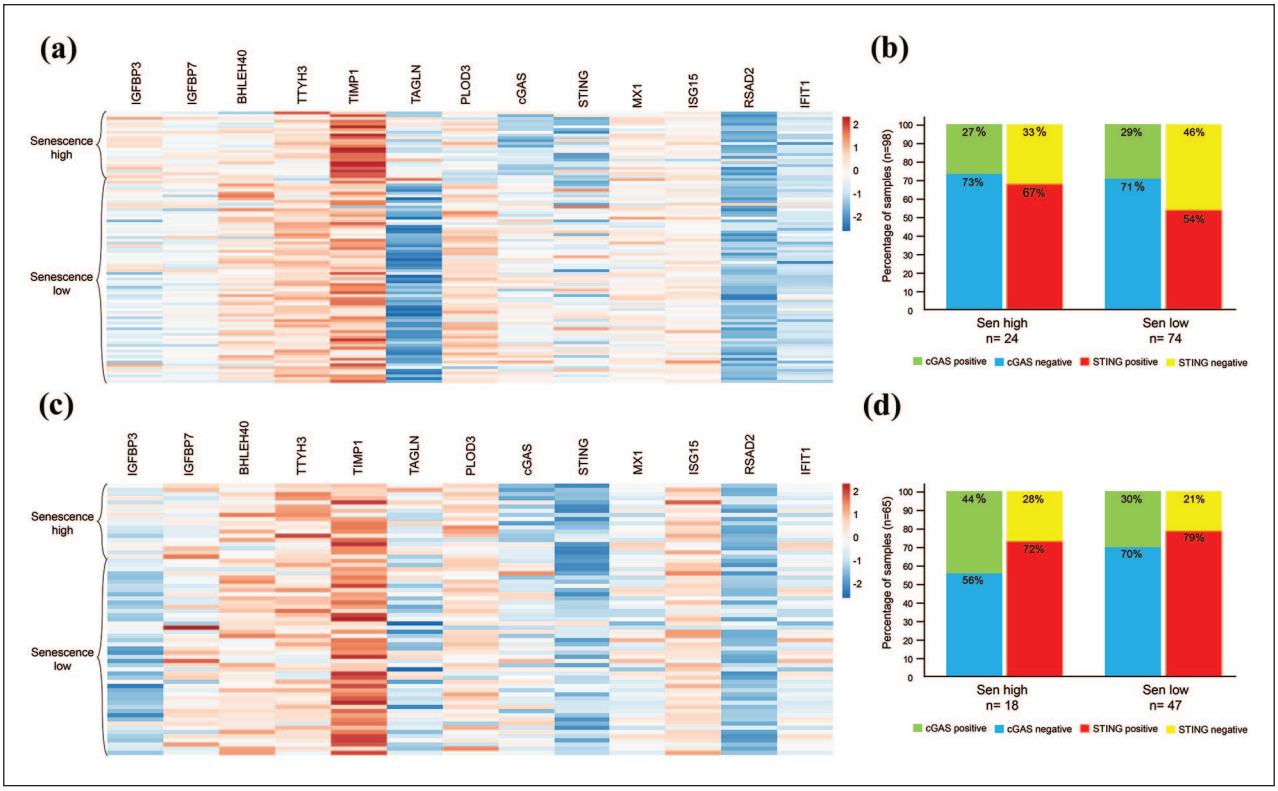

Figure 2. Heatmap and distribution of cGAS/STING and interferon-stimulated gene (ISG) expression in colon cancer relative to senescence signature in two patient cohorts. High senescence was determined by increased expression of *all IGFBP3, IGFBP7, BHLHE40, TTYH3, TIMP1, TAGLN*, and *PLOD3* in cancer relative to the paired non-malignant mucosa. (a) Heatmap of gene expression from GSE44076 ($n = 98$ patients), with 24 patients categorized as high-senescence. (b) Percentage distribution of cGAS and STING positivity (higher in tumor) in high- and low-senescence groups within GSE44076. (c) Heatmap of gene expression from GSE20842 ($n = 65$ patients), identifying 18 patients as high-senescence. (d) Percentage distribution of cGAS and STING positivity (higher in tumor) in high- and low-senescence groups within GSE20842. cGAS and STING expression levels showed no significant correlation with the senescence profile. Similarly, ISGs (*MX1, ISG15, RSAD2, IFIT1*) exhibited variable expression patterns, confirming a lack of association between the senescence signature and cGAS/STING or interferon signaling pathways.
Source: Heatmap was created using ClustVis.[61]

senescence profiling was designed using multiple datasets of colon cancer samples and was demonstrated to be of prognostic value and high reliability for senescence identification in human cancer tissue.[46] Our analysis of the senescence scoring (positive difference tumor to non-malignant tissue for all seven genes) revealed that 25% ($n = 24/98$, GSE44076) and 28% ($n = 18/65$. GSE20842) of colon cancer samples exhibited a "high" senescence expression profile (Figure 2), a percentage close to previously reported levels of senescence in human cancers.[41,59,60]

Unexpectedly, increased cGAS gene expression was found in 71% (17/24) of the GSE44076 samples with "high" senescence profile, which was similar to its expression levels in samples of "low" senescence activity (73%, 54/74) (Figure 2(a and b)). On the other hand, STING expression was found to be higher in tumor tissue in 67% (16/24) of the same samples of "high" senescence profile, while 54% (40/74) of the samples of "low" senescence profile had increased STING gene expression (Figure 2(a and b)). Among the GSE20842 gene set, cGAS expression in tumor tissue was higher in 56% (10/18) and 70% (33/47) of the sample of "high" and "low" senescence profiles, respectively. As for STING, there was higher gene expression in tumor tissue in 28% (5/18) of sample exhibiting a "high" senescence profile and 21% (10/47) of the "low" senescence profile (Figure 2(c and d)). In addition, we performed a Pearson correlation analysis between cGAS, STING, and the seven-gene senescence signature in both datasets and found no significant correlation between cGAS or STING and any of the examined genes (Figure 3(a and b)). Moreover, case-by-case assessment of cGAS/STING expression and the

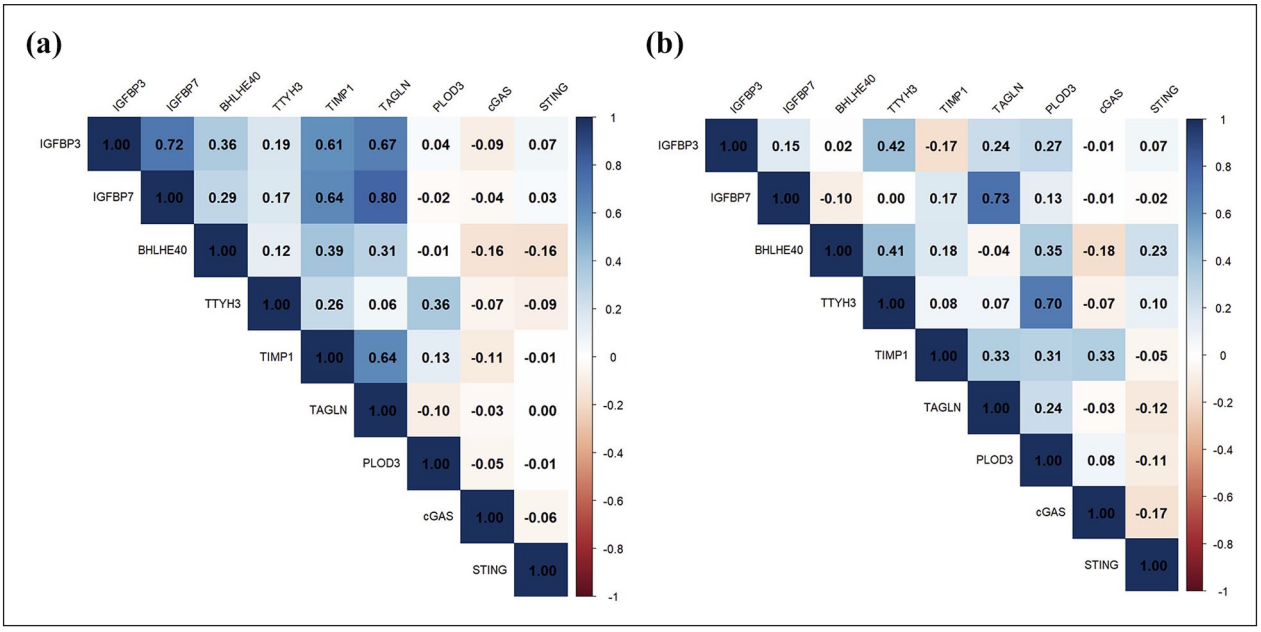

Figure 3. Pearson correlation coefficients between cGAS, STING, and the seven-gene senescence signature across two datasets. No significant correlations were observed between cGAS or STING and any senescence-related genes, indicating a lack of association with senescence status. The color gradient represents correlation strength, with darker blue indicating stronger positive correlations and red indicating stronger negative correlations.

seven-gene senescence signature did not reveal any significant association between cGAS or STING and senescence status (Supplemental Figure 1).

In addition to cGAS/STING, we included four interferon-stimulated genes (ISGs), namely, *MX1*, *ISG15*, *RSAD2*, and *IFIT1*, to explore their association with senescence profiles in colon cancer tissue samples (Figure 2). These genes were selected due to their known role in immune signaling and potential interplay with the cGAS/STING pathway.[62] Heatmap analysis revealed distinct expression patterns of these ISGs across samples with "high" and "low" senescence profiles (Figure 2). Specifically, *MX1*, *ISG15*, *RSAD2*, and *IFIT1* exhibited heterogeneous expression patterns, which were not significantly linked to the seven-gene senescence signature, confirming the lack of association between senescence and cGAS/STING pathway.

Moreover, we performed Gene Set Enrichment Analysis (GSEA) for several cGAS/STING connected pathways and whether any association with the senescence signature can be established. In both the GSE44076 and GSE20842 datasets, the interferon-related pathways exhibited a consistent pattern of negative enrichment across both datasets, albeit with variable statistical significance (Supplemental Table 1). The *interferon-α response pathway* had an NES of −0.86 (FDR q-val = 0.58) and an NES of −1.69 with a marginally significant FDR q-val of 0.04, in GSE44076 and GSE20842, respectively. While within the *interferon-γ response pathway*, GSE44076 showed an NES of −0.66 (FDR q-val = 0.77) and in GSE20842, it displayed an NES of −1.34 (FDR q-val = 0.17). Other pathways were also investigated with only the *Beta-Oxidation of Fatty Acids in Mitochondria Reactome* (which does not have a direct connection to cGAS/STING) demonstrating significant positive enrichment with the senescence signature (Supplemental Table 1).

cGAS is widely expressed in colon cancer

We then validated the protein expression of cGAS/STING in an independent cohort of colon cancer samples. The analysis of cGAS staining revealed that 84% (114/135) of samples had positive staining while 16% (21/135) had negative staining (Table 1). Figure 4 shows representative fields of cGAS/STING staining. STING positivity was found in 36% (48/133) while the remaining 64% (85/133) exhibited negative staining. This suggests that cGAS is widely expressed in colon cancer samples.

Table 1. The correlation between cGAS or STING protein expression levels with the clinicopathological features of the 135 (cGAS) and 133 (STING) colon cancer samples.

Clinicopathological feature	cGAS+	cGAS−	*p*	STING+	STING−	*p*
n =	114 (84%)	21 (16%)		48 (36%)	85 (64%)	
Stage			0.157			0.266
I	11	2		6	5	
II	46	4		20	31	
III	57	15		22	49	
Age			0.816			0.857
⩽63	58	10		24	44	
>63	56	11		24	41	
LN			0.101			0.367
Negative	61	7		27	40	
Positive	53	14		21	45	
LVI			0.056			0.275
Negative	70	8		31	46	
Positive	44	13		17	39	
Differentiation			0.546			0.820
Well	5	0		2	3	
Well to moderate	18	7		7	18	
Moderate	72	13		29	58	
Poor	5	1		2	2	

Cases were defined either as positive or negative based on percentage of positive cells and DAB intensity as detailed within the Methods section. *p* values were calculated using Pearson's Chi-square or Fisher's exact non-parametric tests.
LN: lymph node status; LVI: lymphovascular invasion; *n*: number.

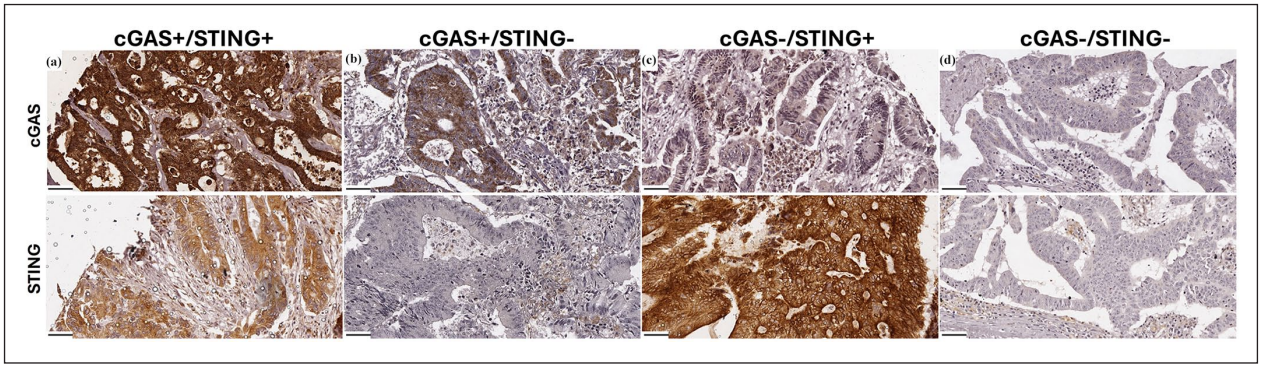

Figure 4. Representative immunohistochemical staining images for cGAS and STING in colonic cancer showing an adenocarcinoma with positive staining in both markers (a), an adenocarcinoma showing positive cGAS staining with negative STING (b), an adenocarcinoma showing positive STING staining with negative cGAS (c) and an adenocarcinoma with negative staining for both markers.

Most of the negative cGAS cases were among stage III samples ($n=15$) compared to stage II ($n=4$) and stage I ($n=2$), however, this difference was of no statistical significance ($p=0.157$). There was no significant difference in the number of positive cGAS samples among the two age groups. Interestingly, the number of positive cGAS cores was the highest among the cases negative for lymph node involvement (LN) ($n=61$) and with no lymphovascular invasion (LVI) ($n=70$), however, with no statistical significance (LN, $p=0.101$; LVI, $p=0.056$). Using the tumor differentiation classification, cGAS was found to be positive in 5 of the 6 poorly-differentiated cases, similarly most of the moderately-differentiated cases were also positive ($n=72$) with only 13 were negative. All cases with well-differentiated tumor were positive for cGAS ($n=5$).

STING protein expression was negative in 49 cases of stage III samples relative to 22 were positive, also 31 were negative in stage II with 20 were

Table 2. The association of the cGAS/STING protein expression with the clinicopathological features of the 124 colon cancer samples.

Clinicopathological feature	cGAS+/STING+	cGAS−/STING−	cGAS+/STING-	cGAS−/STING+	*p*
n =	43	19	60	2	NA
Stage					0.274
I	6	2	3	0	
II	17	4	26	0	
III	20	13	31	2	
Age					0.683
⩽63	23	10	30	0	
>63	20	9	30	2	
LN					0.268
0	24	7	32	0	
1	19	12	28	2	
LVI					0.098
0	29	8	34	0	
1	14	11	26	2	
Differentiation					0.321
Well	2	0	3	0	
Well to moderate	6	6	11	1	
Moderate	25	12	41	1	
Poor	2	1	1	0	

Samples were defined either as positive or negative based on percentage of positive cells and DAB intensity as detailed within the Methods section.
p values were calculated using Pearson's Chi-square or Fisher's exact non-parametric tests.
LN: lymph node status; LVI: lymphovascular invasion; *n*: number.

positive, 6 cases were negative with 5 were positive among stage I cores, however, this was not of statistical significance ($p=0.266$) (Table 1). Similar number of positive STING was observed among the two age groups of 24 cases while 44 and 41 were negative for ⩽63 and >63 years old, respectively. Positive STING staining was observed in 21 and 17 cases that were also positive for LN and LVI, respectively, while 27 and 31 cases of without LN and LVI, respectively, were positive for STING. Numbers of negative STING cases with negative LN and negative LVI were 40 and 46, respectively. However, no statistically significant value was observed with neither LN ($p=0.367$) nor LVI ($p=0.275$). Finally, there was equal number of cases of positive/negative STING among poorly differentiated cases, while 58, 18, and 3 were negative for STING among moderate, well to moderate and well differentiated cores but without statistically significant value ($p=0.820$).

Further analysis of the combined cGAS/STING protein expression in 124 samples showed that 35% (43/124) of the samples were simultaneously positive for both markers, while 15% (19/124) of the samples had negative DAB staining for both proteins. Moreover, 48% (60/124) of the samples had positive cGAS accompanied by negative STING while only 2% (2/124) were vice versa (STING+/cGAS-). Furthermore, analysis of cGAS/STING status with tumor stage, patients' age, lymph node involvement, lymphovascualr invasion and tumor differentiation did not show any statistically significant value as shown in Table 2. These findings of high number of positive cGAS protein expression relative to STING are consistent with the previous findings observed in gene expression analysis. Figure 4 shows the different staining patterns of cGAS/STING in colon cancer tissues.

Discussion

cGAS/STING pathway is a key regulator of the immune response against pathogens and DNA fragments from diseased/cancer cells.[33] Recent preclinical evidence has also demonstrated a strong role for cGAS/STING in regulating senescence and the SASP-mediated immune response against senescent tumor cells.[35,63,64] Unfortunately, the connection between cGAS/STING and senescence has not been examined in clinical cancer samples.

This is largely due to a scarcity of studies that investigated the development of senescence in vivo and the lack of universal biomarkers to identify clinical senescence.[60] In this work, we aimed to profile the gene expression of cGAS/STING in correlation with a previously validated senescence-associated transcriptomic signature in colon cancer tissue using an approach that compares between malignant and non-malignant components of colon tumors. We then validated cGAS/STING expression in an independent cohort of colon cancer samples.

We found that cGAS exhibited increased gene expression in colon cancer samples relative to their matched adjacent non-malignant mucosa in two publicly available gene datasets. Interestingly, around one-quarter of the samples with high cGAS expression exhibited positive (or "high") senescence profile. Among these samples, increased expression of cGAS was found in more than half of the examined samples (71% in GSE44076 and 56% in GSE20842) while STING was higher in 67% (GSE 44076) and 28% (GSE20842) of the non-malignant colonic mucosa samples. Our analyses also did not show any significant association between cGAS, STING, and the seven-gene senescence signature across datasets or on a case-by-case basis. Moreover, no significant enrichment for cGAS/STING related pathways, namely ISGs or interferon response genes (α and γ reactomes) have been identified. Collectively, this suggests a dissociation between the gene expression of cGAS/STING and senescence which, indeed, goes against the emerging preclinical literature that strongly argues for a connection between cGAS/STING and senescence.

This can be due to notable differences in senescence-associated signatures between in vitro and in vivo settings. For example, established markers of in vitro senescence, such as the cell cycle regulators, $p21^{Cip1}$ and $p16^{INK4a}$, can be dissociated from transcriptomic profiles of senescence in vivo.[65] This applies to other hallmarks of senescence including H3K9Me3 or p53.[59,66] Subsequently, this could explain why a stronger connection between cGAS/STING and senescence could not be established in colon cancer. Of course, this certainly does not rule out a role for cGAS/STING in regulating senescence in colon cancer but invites for a more rigorous understanding of in vivo senescence.[37] For this work, we relied on using a previously validated senescence gene expression signature in colon cancer specifically to minimize the variability in senescence development that could arise from cancer background differences.

Using IHC, we further confirmed that cGAS protein is highly expressed in colon cancer in 114 of 135 stained samples while STING had lower frequency of positive staining in 48 of /133. Combined analysis showed that 43 of 124 samples were positive for both markers, while 19 of 124 were negative for IHC staining. Finaly, no statistically significant association was found between cGAS/STING status with various clinicopathological features such as tumor stage, patients' age, lymph node involvement, lymphovascular invasion and tumor differentiation. These findings were not entirely consistent with previous observations. For example, Xia et al. investigated cGAS/STING status in colon cancer using RNA chromogenic in situ hybridization (CISH) ($n=80$) and IHC ($n=40$) and found that 62.5% ($n=50/80$) using CISH and 45% ($n=18/40$) using IHC were positive for both markers while only 9% ($n=7/80$) using CISH and 5% ($n=2/40$) using IHC of samples were negative for the two markers.[42] These findings were similar to ours, in that, we found that 35% of the samples were cGAS+/STING+ and 15% of samples were cGAS-/STING-. Nevertheless, Xia et al. reported higher frequency of cGAS-/STING+ cases compared to cGAS+/STING- using both assays,[42] which is inconsistent with our findings of only 2% of our cohort were cGAS-/STING+ while 48% were the opposite (cGAS+/STING-). Although both studies used the same scoring methods for IHC, defining the cut-off point for IHC positivity was different (we used score >4 while Xia et al., used $\geqslant 3$) which could justify the slight variability in the results. Similar incompatible observations with this study were also reported by Kunac et al. showing low cGAS protein expression in 27/41 (66%) low STING protein expression in 13/41 (32%) of the samples.[67] Furthermore, a recent study explored cGAS/STING in a cohort of 243 colorectal cancer samples and found that 76% and 71% of the samples were negative for cGAS and STING, respectively.[43] In our study, cGAS protein expression was negative in 16% of the samples while STING was not expressed in 64% consistent with Nakajima et al. findings.[43]

The interaction between cGAS/STING pathway and immune regulation was also investigated previously. For example, STING protein

expression in both tumor endothelial cells and immune cells correlates positively with the infiltration of intratumoral CD8+ T cell and was associated with favorable prognosis in two sets of 173 breast and 160 colorectal cancer patients.[68] Similarly, increased CD8+T and CD4+T cells infiltration was associated with increased STING expression, however, cGAS expression was positively associated with only CD8+ T cells, but not CD4+ T cells.[43] These studies suggest that increased expression of cGAS and /or STING is associated with improved clinical outcomes, as evidenced by greater immune cell infiltration and favorable prognosis.[43,68] However, contrasting reports indicate that the cGAS-STING pathway can also activate NF-κB, which may support tumor progression and metastasis by creating an immunosuppressive microenvironment.[69] NF-κB is a key regulator of the SASP as a proteomics analysis of senescent chromatin revealed that the NF-κB influence the expression of more senescence genes than RB and p53 combined.[70]

Our study has several limitations. First, we used TMA which limits the detection of intratumoral heterogeneity due to the presence of non-tumor tissue and tissue folding issue during processing despite its utility in analyzing protein expression and genomic aberrations in relatively large number of samples simultaneously.[38,71,72] Furthermore, a formal sample size calculation was not conducted, which could impact the generalizability of our findings. Another limitation was the inability to obtain normal adjacent tissue samples correlated with the tumor samples due to the fact that some of these samples were more than 15 years old. Lastly, we have not investigated the expression of protein markers of senescence in our independent colon cancer samples primarily due to the lack of a reliable and previously validated senescence-related protein signature.

Conclusions

The expression cGAS/STING is not commensurate with a senescence-associated signature in colon cancer samples in vivo. cGAS expression is higher than STING in malignant components of colon cancer tissue when compared to their non-malignant mucosal counterparts. Positivity of both cGAS and STING protein expression is observed in only one-third of colon cancer samples.

Author contributions

S.A.S and T.S.: Conceptualization, project administration, writing—original draft, data analysis, funding acquisition, supervision; M.E. and A.A.: methodology, immunohistochemical staining; M.R,: data analysis; M.B., E.F.A., and A.M: methodology, constructed TMA; O.A.A.K. and M.A.: methodology, pathological assessment; M.A.A and M.A.Q: Resources; A.I.K., F.N.A, and U.S.: data curation; A.I.K., M.A.Q, M.A.A, M.R.A: editing-original draft. All authors have read and agreed to the published version of the manuscript.

Acknowledgements

All authors are highly thankful to the Researchers Supporting Project number (RSPD2025R786), King Saud University, Riyadh, Saudi Arabia.

Declaration of conflicting interests

The author(s) declared no potential conflicts of interest with respect to the research, authorship, and/or publication of this article.

Funding

The author(s) disclosed receipt of the following financial support for the research, authorship, and/or publication of this article: Sofian Al Shboul (SAS) and Tareq Saleh (TS) are supported by the Deanship of Scientific Research, The Hashemite University (SAS: grants no. 785/48/2022 and 738/54/2022; TS: grants no. 465/83/2019 and 418/84/2019).

Ethics approval

This study was conducted in accordance with the ethical standards set forth in the 1964 Declaration of Helsinki and its subsequent amendments. Ethical approval was obtained from the Institutional Review Board (IRB) of The Hashemite University under the approval number [11/5/2021/2022].

Consent to participate

Obtaining informed consents for this work was waived by the IRB protocols since all the samples used for this study were surplus (archived) tumor tissue samples, and that patients undergoing surgery or biopsy collection provide informed consent to donate any excess tissue (i.e. beyond that needed for clinical purposes).

Informed consent

Obtaining informed consents for this work was waived by the IRB protocols since all the samples used for this study were surplus (archived) tumor tissue samples, and that patients undergoing surgery or biopsy collection provide informed consent to donate any excess tissue (i.e. beyond that needed for clinical purposes).

ORCID iD

Sofian Al Shboul https://orcid.org/0000-0002-0455-4380

Data availability

The patients' datasets generated during the current work are not publicly available due to patients' privacy concerns of the institutional review board policies on human tissue data but are available upon request from the corresponding author.

Supplemental material

Supplemental material for this article is available online.

References

1. Sharpless NE and Sherr CJ (2015) Forging a signature of in vivo senescence. *Nature Reviews Cancer* 15(7): 397–408.
2. Gorgoulis V, Adams PDD, Alimonti A, et al. (2019) Cellular senescence: Defining a path forward. *Cell* 179(4): 813–827.
3. Cho KA, Sung JR, Yoon SO, et al. (2004) Morphological adjustment of senescent cells by modulating caveolin-1 status. *Journal of Biological Chemistry* 279(40): 42270–42278.
4. Son HN, Chi HNQ, Chung DC, et al. (2019) Morphological changes during replicative senescence in bovine ovarian granulosa cells. *Cell Cycle* 18(13): 1490.
5. Miwa S, Kashyap S, Chini E, et al. (2022) Mitochondrial dysfunction in cell senescence and aging. *Journal of Clinical Investigation* 132(13): e158447.
6. Kaplon J, Zheng L, Meissl K, et al. (2013) A key role for mitochondrial gatekeeper pyruvate dehydrogenase in oncogene-induced senescence. *Nature* 498(7452): 109–112.
7. Zglinicki T Von, Saretzki G, Ladhoff J, et al. (2005) Human cell senescence as a DNA damage response. *Mechanisms of Ageing and Development* 126(1): 111–117.
8. Ahmed EK, Rogowska-Wrzesinska A, Roepstorff P, et al. (2010). Protein modification and replicative senescence of WI-38 human embryonic fibroblasts. *Aging Cell* 9(2): 252–272.
9. Fridman AL and Tainsky MA (2008) Critical pathways in cellular senescence and immortalization revealed by gene expression profiling. *Oncogene* 27(46): 5975–5987.
10. Coppé JP, Patil CK, Rodier F, et al. (2008) Senescence-associated secretory phenotypes reveal cell-nonautonomous functions of oncogenic RAS and the p53 tumor suppressor. *PLoS Biology* 6(12): e301.
11. Coppé JPP, Desprez PYY, Krtolica A, et al. (2010) The senescence-associated secretory phenotype: The dark side of tumor suppression. *Annual Review of Pathology: Mechanisms of Disease* 5(1): 99–118.
12. Di Micco R, Fumagalli M, Cicalese A, et al. (2006) Oncogene-induced senescence is a DNA damage response triggered by DNA hyper-replication. *Nature* 444(7119): 638–642.
13. Saleh T, Bloukh S, Carpenter VJ, et al. (2020) Therapy-induced senescence: An "old" friend becomes the enemy. *Cancers (Basel)* 12(4): 822.
14. Collado M, Blasco MA and Serrano M (2007) Cellular senescence in cancer and aging. *Cell* 130(2): 223–233.
15. Prasanna PG, Citrin DE, Hildesheim J, et al. (2021) Therapy-induced senescence: Opportunities to improve anticancer therapy. *Journal of the National Cancer Institute* 113(10): 1285–1298.
16. Reynolds LE, Maallin S, Haston S, et al. (2024) Effects of senescence on the tumour microenvironment and response to therapy. *The FEBS Journal* 291(11): 2306–2319.
17. Lujambio A, Akkari L, Simon J, et al. (2013) Non-cell-autonomous tumor suppression by p53. *Cell* 153(2): 449–460.
18. Mazzoni M, Mauro G, Erreni M, et al. (2019) Senescent thyrocytes and thyroid tumor cells induce M2-like macrophage polarization of human monocytes via a PGE2-dependent mechanism. *Journal of Experimental & Clinical Cancer Research* 38(1): 1–16.
19. Abu-Humaidan AHAH, Ismail MA, Ahmad FM, et al. (2024) Therapy-induced senescent cancer cells exhibit complement activation and increased complement regulatory protein expression. *Immunology & Cell Biology* 102(4): 240–255.
20. Wu M, Han J, Wu H, et al. (2023) Proteasome-dependent senescent tumor cells mediate immunosuppression through CCL20 secretion and M2 polarization in pancreatic ductal adenocarcinoma. *Frontiers in Immunology* 14: 1216376.
21. Iannello A and Raulet DH (2014) Immunosurveillance of senescent cancer cells by natural killer cells. *Oncoimmunology* 3(1): e27616.
22. Kale A, Sharma A, Stolzing A, et al. (2020) Role of immune cells in the removal of deleterious senescent cells. *Immunity & Ageing* 17(1): 1–9.
23. Ortiz-Montero P, Londoño-Vallejo A and Vernot JP (2017) Senescence-associated IL-6 and IL-8 cytokines induce a self- and cross-reinforced senescence/inflammatory milieu strengthening tumorigenic capabilities in the MCF-7 breast cancer cell line. *Cell Communication and Signaling* 15(1): 1–18.
24. Xu Q, Long Q, Zhu D, et al. (2019) Targeting amphiregulin (AREG) derived from senescent stromal cells diminishes cancer resistance and averts programmed cell death 1 ligand (PD-L1)-mediated immunosuppression. *Aging Cell* 18(6): e13027.

25. Ruhland MK and Alspach E (2021) Senescence and immunoregulation in the tumor microenvironment. *Frontiers in Cell and Developmental Biology* 9: 754069.
26. Ye J, Huang X, Hsueh EC, et al. (2012) Human regulatory T cells induce T-lymphocyte senescence. *Blood* 120(10): 2021–2031.
27. Takasugi M, Yoshida Y and Ohtani N (2022) Cellular senescence and the tumour microenvironment. *Molecular Oncology* 16(18): 3333–3351.
28. Pereira BI, Devine OP, Vukmanovic-Stejic M, et al. (2019) Senescent cells evade immune clearance via HLA-E-mediated NK and CD8+ T cell inhibition. *Nature Communications* 10(1): 1–13.
29. Zhou J, Zhuang Z, Li J, et al. (2023). Significance of the cGAS-STING pathway in health and disease. *International Journal of Molecular Sciences* 24(17): 13316.
30. Decout A, Katz JD, Venkatraman S, et al. (2021). The cGAS-STING pathway as a therapeutic target in inflammatory diseases. *Nature Reviews Immunology* 21(9): 548–569.
31. Yang H, Wang H, Ren U, et al. (2017) cGAS is essential for cellular senescence. *Proceedings of the National Academy of Sciences of the United States of America* 114(23): E4612–E4620.
32. Schmitz CRR, Maurmann RM, Guma FTCR, et al. (2023). cGAS-STING pathway as a potential trigger of immunosenescence and inflammaging. *Frontiers in Immunology* 14: 1132653.
33. Li T and Chen ZJ (2018). The cGAS-cGAMP-STING pathway connects DNA damage to inflammation, senescence, and cancer. *Journal of Experimental Medicine* 215(5): 1287–1299.
34. Glück S, Guey B, Gulen MF, et al. (2017) Innate immune sensing of cytosolic chromatin fragments through cGAS promotes senescence. *Nature Cell Biology* 19(9): 1061–1070.
35. Paffenholz SV, Salvagno C, Ho YJ, et al. (2022) Senescence induction dictates response to chemo- and immunotherapy in preclinical models of ovarian cancer. *Proceedings of the National Academy of Sciences of the United States of America* 119(5): e2117754119.
36. Dou Z, Ghosh K, Vizioli MG, et al. (2017) Cytoplasmic chromatin triggers inflammation in senescence and cancer. *Nature* 550(7676): 402–406.
37. Elshazly AM, Shahin U, Al Shboul S, et al. (2024). A Conversation with ChatGPT on contentious issues in senescence and cancer research. *Molecular Pharmacology* 105(5): 313–327.
38. Al Shboul S, Curran OEOEOE, Alfaro JAJA, et al. (2021) Kinomics platform using GBM tissue identifies BTK as being associated with higher patient survival. *Life Science Alliance* 4(12): e202101054.
39. Al Shboul S, Boyle S, Singh A, et al. (2024) FISH analysis reveals CDKN2A and IFNA14 co-deletion is heterogeneous and is a prominent feature of glioblastoma. *Brain Tumor Pathology* 41(1): 4–17.
40. Saleh T, Alhesa A, El-Sadoni M, et al. (2022) The expression of the senescence-associated biomarker lamin B1 in human breast cancer. *Diagnostics (Basel, Switzerland)* 12(3): 609.
41. El-Sadoni M, Shboul SA, Alhesa A, et al. (2023) A three-marker signature identifies senescence in human breast cancer exposed to neoadjuvant chemotherapy. *Cancer Chemotherapy and Pharmacology* 91(4): 345–360.
42. Xia T, Konno H, Ahn J, et al. (2016). Deregulation of STING signaling in colorectal carcinoma constrains DNA damage responses and correlates with tumorigenesis. *Cell Reports* 14(2): 282–297.
43. Nakajima S, Kaneta A, Okayama H, et al. (2023) The impact of tumor cell-intrinsic expression of cyclic GMP-AMP synthase (cGAS)-stimulator of interferon genes (STING) on the infiltration of CD8+ T cells and clinical outcomes in mismatch repair proficient/microsatellite stable colorectal cancer. *Cancers (Basel)* 15(10): 2829.
44. Edgar R, Domrachev M and Lash AE (2002) Gene expression omnibus: NCBI gene expression and hybridization array data repository. *Nucleic Acids Research* 30(1): 207–210.
45. Sanz-Pamplona R, Berenguer A, Cordero D, et al (2014) Aberrant gene expression in mucosa adjacent to tumor reveals a molecular crosstalk in colon cancer. *Molecular Cancer* 13(1): 1–19.
46. Gaedcke J, Grade M, Jung K, et al. (2010) Mutated KRAS results in overexpression of DUSP4, a MAP-kinase phosphatase, and SMYD3, a histone methyltransferase, in rectal carcinomas. *Genes, Chromosomes & Cancer* 49(11): 1024–1034.
47. Subramanian A, Tamayo P, Mootha VK, et al. (2005) Gene set enrichment analysis: A knowledge-based approach for interpreting genome-wide expression profiles. *Proceedings of the National Academy of Sciences of the United States of America* 102(43): 15545–15550.
48. McKinney W (2010) Data structures for statistical computing in python. *SciPy* 445(1): 51–56.
49. Lv MYY, Cai D, Li CHH, et al. (2023) Senescence-based colorectal cancer subtyping reveals distinct molecular characteristics and therapeutic strategies. *MedComm* 4(4): e333.
50. Fang Z, Liu X and Peltz G (2023) GSEApy: A comprehensive package for performing gene set enrichment analysis in Python. *Bioinformatics* 39(1): btac757.
51. Mootha VK, Lindgren CM, Eriksson KF, et al. (2003) PGC-1alpha-responsive genes involved in oxidative

phosphorylation are coordinately downregulated in human diabetes. *Nature Genetics* 34(3): 267–273.
52. Benjamini Y and Hochberg Y (1995) Controlling the false discovery rate: A practical and powerful approach to multiple testing. *Journal of the Royal Statistical Society Series B: Statistical Methodology* 57(1): 289–300.
53. Debacq-Chainiaux F, Pascal T, Boilan E, et al. (2008). Screening of senescence-associated genes with specific DNA array reveals the role of IGFBP-3 in premature senescence of human diploid fibroblasts. *Free Radical Biology and Medicine* 44(10): 1817–1832.
54. Hong S and Kim MM (2018) IGFBP-3 plays an important role in senescence as an aging marker. *Environmental Toxicology and Pharmacology* 59: 138–145.
55. Siraj Y, Aprile D, Alessio N, et al. (2024). IGFBP7 is a key component of the senescence-associated secretory phenotype (SASP) that induces senescence in healthy cells by modulating the insulin, IGF, and activin A pathways. *Cell Communication and Signaling* 22(1): 540.
56. Xu Q, Ma P, Hu C, et al. (2012) Overexpression of the DEC1 protein induces senescence in vitro and is related to better survival in esophageal squamous cell carcinoma. *PLoS One* 7(7): e41862.
57. Guccini I, Revandkar A, D'Ambrosio M, et al. (2021) Senescence reprogramming by TIMP1 deficiency promotes prostate cancer metastasis. *Cancer Cell* 39(1): 68–82.e9.
58. Kim TR, Lee HM, Lee SY, et al. (2010) SM22α-induced activation of p16INK4a/retinoblastoma pathway promotes cellular senescence caused by a subclinical dose of γ-radiation and doxorubicin in HepG2 cells. *Biochemical and Biophysical Research Communications* 400(1): 100–105.
59. Saleh T, Alhesa A, Al-Balas M, et al. (2021) Expression of therapy-induced senescence markers in breast cancer samples upon incomplete response to neoadjuvant chemotherapy. *Bioscience Reports* 41(5): BSR20210079.
60. Saleh T, Bloukh S, Hasan M, et al. (2023) Therapy-induced senescence as a component of tumor biology: Evidence from clinical cancer. *Biochimica et Biophysica Acta (BBA)* 1878(6): 188994.
61. Metsalu T and Vilo J (2015) ClustVis: A web tool for visualizing clustering of multivariate data using principal component analysis and heatmap. *Nucleic Acids Research* 43(W1): W566–70.
62. Schoggins JW and Rice CM (2011) Interferon-stimulated genes and their antiviral effector functions. *Current Opinion in Virology* 1(6): 519–525.
63. Kong SH, Ma L, Yuan Q, et al. (2023) Inhibition of EZH2 alleviates SAHA-induced senescence-associated secretion phenotype in small cell lung cancer cells. *Cell Death Discovery* 9(1): 1–12.
64. Wang T, Liu W, Shen Q, et al. (2023) Combination of PARP inhibitor and CDK4/6 inhibitor modulates cGAS/STING-dependent therapy-induced senescence and provides "one-two punch" opportunity with anti-PD-L1 therapy in colorectal cancer. *Cancer Science* 114(11): 4184–4201.
65. Hernandez-Segura A, de Jong TV., Melov S, et al. (2017). Unmasking transcriptional heterogeneity in senescent cells. *Current Biology* 27(17): 2652–2660.e4.
66. te Poele RH, Okorokov AL, Jardine L, et al. (2002). DNA damage is able to induce senescence in tumor cells in vitro and in vivo. *Cancer Research* 62(6): 1876–1883.
67. Kunac N, Degoricija M, Viculin J, et al. (2023) Activation of cGAS-STING pathway is associated with MSI-H stage IV colorectal cancer. *Cancers (Basel)* 15(1): 221.
68. Yang H, Lee WS, Kong SJ, et al. (2019) STING activation reprograms tumor vasculatures and synergizes with VEGFR2 blockade. *Journal of Clinical Investigation* 129(10): 4350–4364.
69. Jiang M, Jiang M, Chen P, et al. (2020) cGAS-STING, an important pathway in cancer immunotherapy. *Journal of Hematology & Oncology* 13(1): 1–11.
70. Chien Y, Scuoppo C, Wang X, et al. (2011) Control of the senescence-associated secretory phenotype by NF-κB promotes senescence and enhances chemosensitivity. *Genes & Development* 25(20): 2125–2136.
71. Kündig P, Giesen C, Jackson H, et al. (2018) Limited utility of tissue micro-arrays in detecting intratumoral heterogeneity in stem cell characteristics and tumor progression markers in breast cancer. *Journal of Translational Medicine* 16(1): 118.
72. Nassar A, Radhakrishnan A, Cabrero IA, et al. (2010). Intratumoral heterogeneity of immunohistochemical marker expression in breast carcinoma: A tissue microarray-based study. *Applied Immunohistochemistry & Molecular Morphology* 18(5): 433–441.